Solid State Phenomena
ISSN: 1662-9779, Vol. 388, pp 73-79
doi:10.4028/p-W8FBjz

Submitted: 2026-01-08
Revised: 2026-02-16
Accepted: 2026-02-21
Online: 2026-04-15

Investigating the Formability of Aluminium Alloy Tubes by Rubber Bulge Testing

Chanmi Moon[1,a*], Eren Can Sariyarlioglu[1,b] and Torgeir Welo[1,c]

[1]Norwegian University of Science and Technology, Trondheim, Norway

[a*]chanmi.moon@ntnu.no, [b]eren.c.sariyarlioglu@ntnu.no, [c]torgeir.welo@ntnu.no

Keywords: Al-Mg-Si alloy, extrusion, rubber bulge testing, formability.

Abstract. Efficient characterization of formability of tubular sections is essential for designing lightweight aluminum extrusion components, particularly since the presence of weld seams and extrusion-induced inhomogeneities influence deformation behavior. This study evaluates the formability of Al–Mg–Si alloy tubes after being subjected to four different heat-treatment conditions, using a non-conventional rubber-assisted bulge test. A solid polyurethane (PU) plug was employed as pressure medium to enable full-scale deformation. Digital image correlation (DIC) was used to quantify circumferential and longitudinal strain evolutions, while post-fracture thickness measurements provided complementary insight into through-thickness strain. The measured circumferential strain at fracture ranged from 0.15 to 0.24 across the investigated tempers. The W-tempered condition exhibited the highest surface strain while maintaining moderate thickness reduction, whereas the soft-annealed tubes showed the largest thinning. These results demonstrate that tube formability, as evaluated by the present testing approach, is characterized by the combined evolution of surface strain and thickness reduction, both of which are influenced by heat treatment. Overall, the study shows that PU-assisted rubber bulge testing provides a practical and robust experimental framework for the comparative assessment of formability in extruded aluminum tubes.

Introduction

Aluminum alloy extrusions are widely used in automotive, transportation, and structural applications where lightweight design, crash performance and manufacturing efficiency are critical. Hollow, tubular-type profiles in particular combine low weight with favorable structural integrity and geometric flexibility, which makes them suitable for components subjected to bending, torsion and different multi-axial loading conditions. However, their deformation characteristics can be strongly affected by extrusion process-related factors such as seam welds, thickness variations and microstructural heterogeneities [1]. For forming-intensive processes, therefore, an accurate, practical and application-relevant assessment method for tube formability is therefore essential.

While conventional tensile testing provides standardized material data, it offers limited relevance for tubular geometries where multiple factors play a decisive role. Bulge-based formability tests have consequently received increased attention as means to characterize deformation behavior under more realistic boundary conditions. Traditional bulge tests typically use hydraulic pressurization [2-3], but alternative test concepts have been introduced to simplify operation and enable evaluation at component level. A particular bulge approach uses a solid rubber mandrel that expands under axial compression, inducing internal pressure through the Poisson effect of the rubber [4]. This configuration allows testing without complex fluid-handling systems. Recent studies have demonstrated that, among different material alternatives, solid polyurethane (PU) provide stable and reproducible deformation characteristics [5], which makes it a suitable pressure medium in tube bulging.

In this work, the PU-based rubber bulge method is applied to assess the formability of circular Al–Mg–Si alloy tubes which have been subjected to different heat-treatment routes.

By combining load–displacement measurements with full-field strain analysis via digital image correlation (DIC), the study investigates how temper condition influences the deformation capacity, fracture behavior and overall structural response of pressurized extruded tubes. Particular attention is given to major circumferential strain development and post-fracture thickness distribution.

Experimental Methods

Materials

The Al–Mg–Si alloy tubes were supplied in a partially solutionized condition resulting from the extrusion process itself. Although extrusion under appropriate thermal conditions can ideally produce a fully solutionized state, complete solutionization was not achieved in the present material. Therefore, this condition is herein referred to as the as-received or partially solutionized condition (PS). The chemical composition of the tubes is listed in Table 1.

For subsequent heat treatments, the tubes were solution heat-treated at 565 °C for 1 h followed by water quenching (WT). Natural ageing (NA) was achieved for T4 temper by storing the quenched tubes at room temperature for one week. For the soft annealed temper (SA), the tubes were annealed in a furnace at 410 °C for 4–6 h (Fig. 1(a)). Formability tests were conducted within 15 min after quenching to preserve the supersaturated solid-solution state characteristic of freshly quenched material.

The tubes had an outer diameter of 60 mm, an average wall thickness of 2 mm. They were delivered as 1,000 mm-long hollow circular extrusions, which were later cut into 150 mm sections for testing. A solid polyurethane (PU) rubber block was employed as the pressure medium. The hardness of PU block is 90 Shore, according to rubber supply. The block was fabricated using waterjet cutting into a cylindrical shape with a nominal diameter of 50 mm and a length of 100 mm (Fig. 1(b)).

Table 1. Chemical compositions of Al-Mg-Si extrusion profile in use (weight %).

Al	Mg	Si	Mn	Cr	Fe	Zn	Cu	Ti
97.5	1.00	0.66	0.08	0.06	0.22	0.405	0.0025	0.09

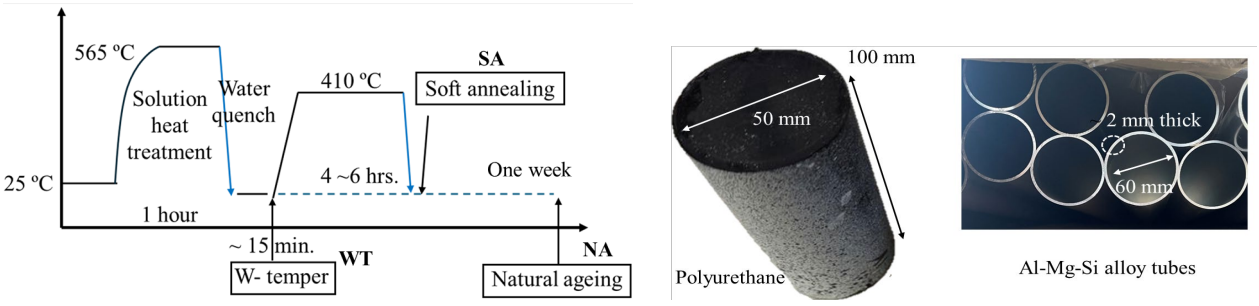

(a) (b)

Fig. 1. (a) Heat-treatment history for producing the different tube tempers. (b) Geometry of PU rubber block used as the pressure medium in the bulge tests and tube that have been tested.

Rubber bulge testing

All rubber-based bulge tests were conducted using an Instron 8854 hydraulic compression system with a 250 kN load capacity. A solid rubber plug was positioned inside the aluminum alloy tube between the upper punch and the fixed lower support, as schematically shown in Fig. 2(a). After ensuring proper alignment, the rubber was compressed at a constant ram speed of 0.5 mm/s, generating internal pressure that induced circumferential expansion of the tube until fracture. The full experimental setup, including the punch and die arrangement, is presented in Fig. 2(b).

The specimen geometry was designed to minimize potential sources of experimental disturbance. To prevent the centering rims at each tube end from affecting the deformation response, their lengths were selected to exceed the tube diameter, ensuring the presence of an undeformed region outside the transition zone. Additionally, the effective specimen length was set to approximately twice the tube diameter-following the recommendations of Donati et al. [4]-to promote uniform deformation of the rubber plug and avoid buckling. As a result, the rubber plug length and total specimen length were defined as 100 mm and 150 mm, respectively.

Before testing, the inner surface of each tube was lubricated with spray-type WD-40 PTFE lubricant to minimize friction between the punches, the rubber plug and the specimen. The displacement at instant of fracture and load were determined from the recorded load–displacement curves. For deformation analysis, stereo system digital image correlation (DIC), which accounts for out-of-plane deformation, was applied to the tube surface during testing (Fig. 2(c)) to quantify circumferential and longitudinal strain fields and determine local fracture strain. Both point analysis and virtual extensometer measurements were performed and found to correspond closely, hence validating the measurement approach. Consequently, point analysis was used for fracture strain characterization, averaging the measured strains from three to five points adjacent to the fracture site. Each test was repeated three times and the reported results represent the average values.

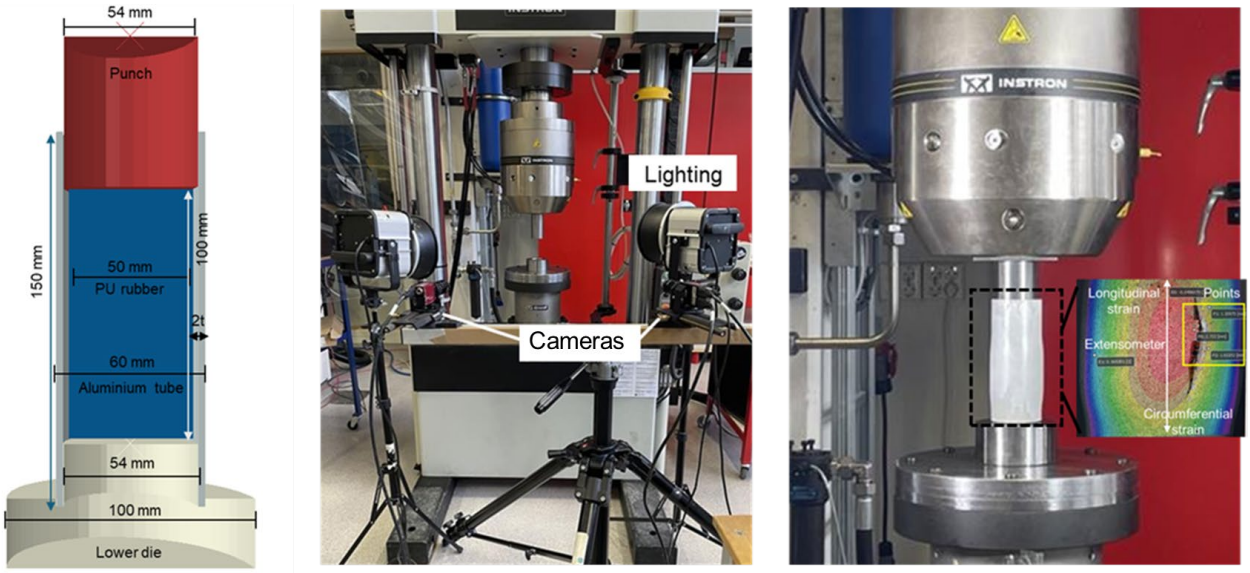

(a) (b) (c)

Fig. 2. (a) Schematic of the rubber-based bulge test setup. (b) Experimental setup with punch and die arrangement. (c) DIC application for surface strain measurement during testing.

Results and Discussion

Loading curve comparison

A representative load–stroke curve obtained from a bulge test is presented in Fig. 3(a), where three distinct deformation stages can be identified. The punch displacement is plotted in descending order, from 20 mm to −20 mm, to reflect the compressive nature of the test.

In the initial stage (Stage I), corresponding to a punch stroke between 20 mm and 0 mm, the load increases linearly with a constant slope, representing the initial response of the polyurethane (PU) rubber plug. During the second stage (Stage II), the load rises linearly with a steeper slope, indicating the onset of deformation in the metallic tube. In the third stage (Stage III), a further change in slope occurs as the tube material deforms into the plastic region. The load continues to increase during this phase until reaching its maximum value, at which point the test is terminated. Beyond this peak load, a rapid load drop is observed, signifying fracture of the tube wall.

Figure 3(b) compares the average punch displacement and the maximum load of specimens subjected to the different heat-treatment conditions. The PS tube exhibited the lowest punch displacement and the highest fracture load. In contrast, the water-tempered (WT) specimen showed a significantly higher punch displacement and a lower maximum load. Specifically, the WT condition reached approximately 75% of the peak load of the as received/partially solutionized (PS) tube (41 kN vs. 55 kN) while achieving about a 17% increase in punch displacement (20.0 mm vs. 17.8 mm). The naturally aged specimen (NA) demonstrated a slight increase in punch displacement and a modest reduction in maximum load relative to the PS state. The soft-annealed samples, consistent with the significantly lower loading curve in Fig. 3(a), exhibited the largest punch displacement of all conditions, approximately 120% of the as-received PS tubes displacement—and only about 65% of its maximum load. A summary of these results is provided in Table 2. In this table, d^* is the punch displacement at fracture, $f_{\max}$ is the maximum punch force, and $\bar{\varepsilon}^*$ is the average circumferential fracture strain measured by Stereo-DIC near the fracture site.

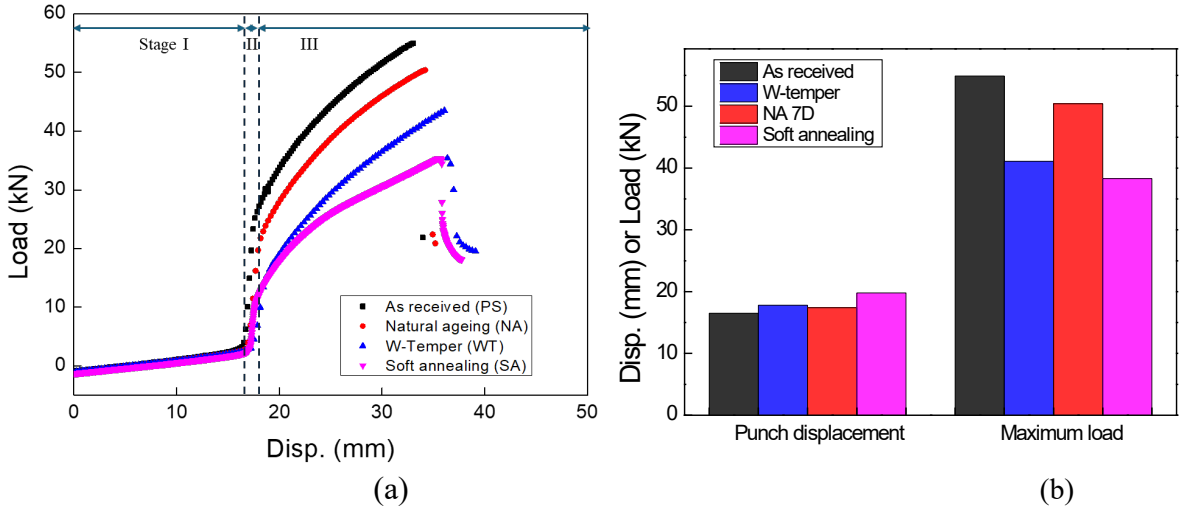

(a) (b)

Fig. 3. (a) Load–displacement curves for the different tempers. (b) Comparison of maximum load and punch displacement at fracture.

Table 2. Summary of maximum load and punch displacement for all heat-treatment conditions.

Temper	Loading curve		DIC
	d^* (mm)	$f_{\max}$ (kN)	$\overline{\varepsilon^*}$
As received (Partially solutionized, PS)	16.5	54.9	0.15
Natural ageing (NA)	17.4	50.4	0.17
W- temper (WT)	18.6	43.4	0.24
Soft annealing (SA)	19.8	38.3	0.21

DIC strain analysis

Digital image correlation (DIC) was employed to characterize the deformation behavior of the tubes during bulge testing. Strain fields (Fig. 2(c)) were recorded across the entire observable surface, as captured by the camera setup in Fig. 2(b). Since bulging induces dominant circumferential expansion and comparatively minor axial stretching [6], the former was treated as the major strain component (Fig. 4(a)). Strain values were extracted in both directions and monitored throughout the test, with particular emphasis on points located adjacent to the eventual fracture region to ensure that the peak deformation state was accurately captured.

Figure 4(b) presents the major circumferential strain at fracture for each temper condition. The PS tube exhibited the lowest major strain, approximately 0.15, reflecting its higher strength and more limited ductility also seen in the load–displacement response. The naturally aged condition (NA)

showed a slightly higher strain of 0.17, indicating a modest increase in deformation capacity. The water-tempered (WT) condition displayed a substantially larger major strain of 0.24, also reflected by its higher punch displacement and reduced peak load. Finally, the soft-annealed tubes exhibited a fracture strain of 0.21, which is lower than that of the WT condition but significantly higher than that of the PS and NA samples. This aligns with the pronounced softening observed in the annealed condition, where the loading curve indicates reduced work-hardening and enhanced ductility.

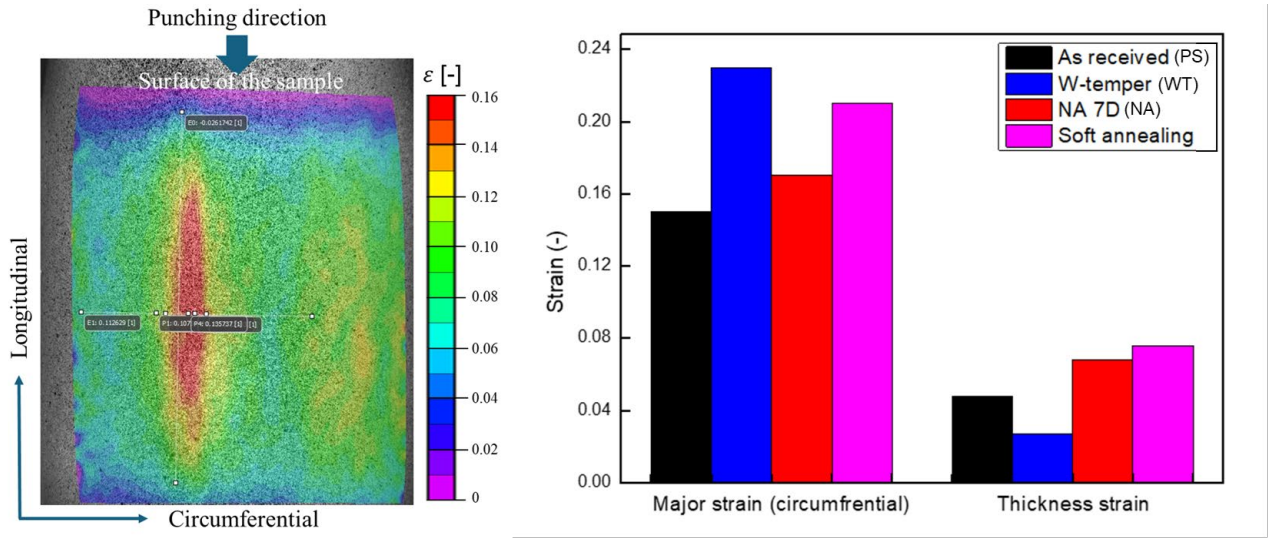

(a) (b)

Fig. 4. (a) DIC view of sample surface with selected measurement points for strain analysis. (b) Comparison of circumferential major strain and thickness stain at fracture for all heat-treatment conditions, obtained from DIC analysis.

Thickness distribution measurement

To evaluate the thickness evolution during bulging, specimens were sectioned along the longitudinal mid-plane through the fracture zone using a bandsaw. The resulting cross-sections were measured manually with a vernier caliper and a micrometer (Fig. 5(a)). As shown by the thickness distribution of the as received (PS) material, the tube thickness was not uniform but varied with circumferential angle. Consequently, thickness values were not derived from DIC measurements, which would beneficial with volume conservation assumption, but were instead determined directly from physical measurements. Thickness was recorded at 15° intervals over the full circumferential range from −180° to 180°, enabling accurate mapping of the thickness distribution in the fracture region. Because the PS tubes exhibited inherent circumferential thickness variations originating from the extrusion process (Fig. 5(b)), the undeformed thickness profile was documented in advance to ensure that deformation-induced thickness changes could be correctly referenced at corresponding angular positions.

Comparison of the thickness distributions revealed noticeable differences among the temper conditions (Fig. 5(c)). The soft-annealed tube exhibited the largest thickness reduction, which appears consistent with its reduced load-bearing capacity and the high deformation levels observed. This behavior may suggest a lower resistance to thinning associated with its fully softened mechanical state [7]. In contrast, the WT condition showed only moderate thickness reduction, despite exhibiting the highest major strain in the DIC analysis. This observation suggests that, under the deformation mode investigated in this study, the solution heat-treated WT condition may retain a comparatively higher resistance to thinning, potentially related to its mechanical response and the presence of a supersaturated solid-solution microstructure, as reported in previous studies [8-10]. The naturally aged and as-received (PS) tubes displayed similar thickness distributions, which may reflect comparable work-hardening behavior and load responses, in agreement with the trends shown in Fig. 3(a).

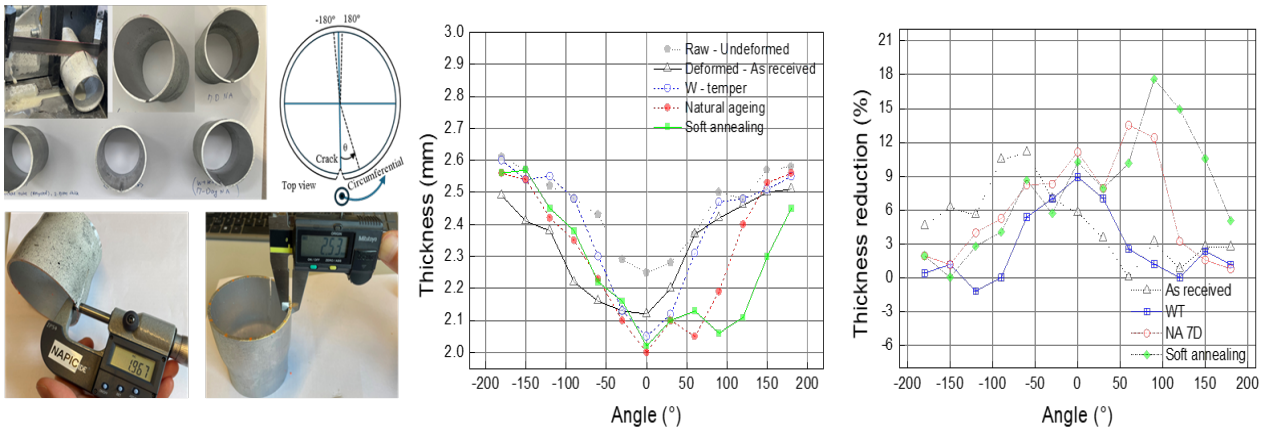

(a) (b) (c)

Fig. 5. (a) Thickness-measurement procedure on the fractured tube section. (b) Measured circumferential thickness distributions for all temper conditions. (c) Corresponding thickness-reduction profiles as a function of circumferential angle.

Interpretation and formability implications

Overall, the DIC and thickness-reduction results highlight distinct deformation responses among the heat-treatment conditions investigated. The WT tube exhibited the highest surface strain while maintaining only moderate thinning, indicating a deformation response in which substantial in-plane stretching occurred without a proportional increase in thickness reduction. In contrast, the soft-annealed tube—although capable of large overall deformation—showed pronounced thinning, which can be associated with its lower strength level and limited work-hardening capacity. The as-received (PS) tubes displayed both lower major strains and moderate thinning, suggesting a more restricted deformation capability. A similar response was observed for the naturally aged condition.

Taken together, these results suggest that tube formability, as assessed by the rubber bulge forming approach used in this study, is influenced by the concurrent development of surface strain and thickness reduction, rather than by either metric alone. While this interplay is inherent to tube deformation, the present results demonstrate how different heat-treatment conditions manifest distinct combinations of these responses under identical loading conditions. For the WT condition, the observed combination of high surface strain and moderate thinning may be associated with its specific mechanical state and microstructural condition, as reported in the literature [9–11]. However, further targeted studies would be required to establish a direct link between solute content, hardening state, and thinning resistance.

From an application perspective, the results indicate that selecting an appropriate temper has the potential to influence the balance between achievable expansion and thickness stability in tubular extrusions. Rather than implying direct process optimization, the present findings provide comparative insights that may support future efforts aimed at tailoring heat-treatment routes for deformation modes relevant to energy absorption or forming performance.

Summary

Based on the results obtained in this experimental study, the following can be summarized:

- The PU-assisted rubber bulge tests serve comparative tube formability characterization.
- The WT tubes exhibited the highest circumferential strain at fracture.
- The soft-annealed tubes showed the largest thickness reduction.
- Tube formability was characterized by the coupled surface strain and thickness reduction.

References

[1] Reggiani, B., Segatori, A., Donati, L., Tomesani, L., Terenzi, A., & Salice, A. (2014). Comparison of bulge test vs. conical expansion test for hollow extruded profile characterization. *Key Engineering Materials*, *585*, 111-119.

[2] Thiruvarudchelvan, S., Seet, G. L., & Ang, H. E. (1996). Computer-monitored hydraulic bulging of tubes. *Journal of materials processing technology*, *57*(1-2), 182-188.

[3] Sokolowski, T., Gerke, K., Ahmetoglu, M., & Altan, T. (2000). Evaluation of tube formability and material characteristics: hydraulic bulge testing of tubes. *Journal of Materials Processing Technology*, *98*(1), 34-40.

[4] Reggiani, B., & Donati, L. (2020). Comparison of experimental methods to evaluate seam welds quality in extruded profiles. *Transactions of Nonferrous Metals Society of China*, *30*(3), 619-634.

[5] Yang, J., Li, H., Huang, D., Li, G., & Yuan, S. (2020). Forming of thin-walled AA6061-T4 tubular joint by elastomeric bulging: experiment and computation. *The International Journal of Advanced Manufacturing Technology*, *107*(1), 25-38.

[6] Chu, E., & Xu, Y. (2004). Hydroforming of aluminum extrusion tubes for automotive applications. Part I: buckling, wrinkling and bursting analyses of aluminum tubes. *International journal of mechanical sciences*, *46*(2), 263-283.

[7] Li, Y., Wang, Q. P., Gao, G. J., Li, J. D., Wang, Z. D., & Xu, G. M. (2019). Texture evolution and mechanical properties of Al–Mg–Si alloys at different intermediate annealing temperatures. *Rare Metals*, *38*(10), 937-945.

[8] Zhang, R., Wang, W., & Jiang, J. (2025). Precipitation hardening: Unravelling mechanisms of trade-off between strength and ductility/formability of Al-Mg-Si alloys. *Journal of Alloys and Compounds*, *1012*, 178443.

[9] Zheng, K., Zhu, L., Lin, J., Dean, T. A., & Li, N. (2019). An experimental investigation of the drawability of AA6082 sheet under different elevated temperature forming processes. *Journal of Materials Processing Technology*, *273*, 116225.

[10] Moon, C., Thuillier, S., Lee, J., & Lee, M. G. (2021). Mechanical properties of solution heat treated Al-Zn-Mg-Cu (7075) alloy under different cooling conditions: Analysis with full field measurement and finite element modeling. Journal of Alloys and Compounds, 856, 158180.

[11] Chen, L., Yuan, S., Kong, D., Zhao, G., He, Y., & Zhang, C. (2019). Influence of aging treatment on the microstructure, mechanical properties and anisotropy of hot extruded Al-Mg-Si plate. *Materials & Design*, *182*, 107999.